Steady states in cavity QED due to incoherent pumping

G. S. Agarwal and S. Dutta Gupta
School of Physics, University of Hyderabad, Hyderabad 500134, India
(Received 20 February 1990)

It is shown that strong competition between the absorption and emission of the cavity photons and the incoherent processes like atomic spontaneous emission and cavity decay effects result in new nonequilibrium states in cavity quantum electrodynamics. Such states can exhibit saturation, nonclassical character, and strong atom cavity-correlation.

The strong coupling of the atom with the cavity mode leads to important modifications of the radiation produced by excited atoms in the cavities.[1-8] For example, the linear response[5] shows vacuum-field Rabi splittings.[4,5,8] Other consequences of the strong coupling are, for example, the possibility of very-low-threshold laser action in microcavities[9] and the possibility of changing the nature of the nonlinearity generated signals.[7] Much of the previous work has either considered the interaction of the excited atoms in the absence of pumps or treated the pump in a perturbative way. In this paper we study the interaction of strongly pumped atoms with the microcavities. We model the pumping as an incoherent process and derive *exact* results for the steady-state behavior of the coupled atom-cavity system. We show how the strong coupling can produce new nonequilibrium states depending on the pumping rate and the coupling constant. We exhibit saturation of the photon numbers with increased atom-cavity coupling. The strong negative correlation between the atom and field is demonstrated. The response function of the cavity at various detunings is obtained. The response curve broadens as the cavity-atom coupling increases, which is reminiscent of power-broadening phenomena in semiclassical resonance physics.

Consider a two-level atom pumped by an external radiation in an optical cavity. Let the pump field with frequency ω_c be in resonance with the cavity mode that is described by the boson operators a and $a^\dagger$. Let the atom with the transition frequency ω_0 be characterized by the spin-half operators $S^\pm$ and S^z. The atom-field interaction in the presence of cavity decay given by decay constant κ and other atomic relaxation processes can be described by the master equation

$$\frac{\partial\rho}{\partial t}=-i\delta[S^z,\rho]-ig[(S^+a+S^-a^\dagger),\rho]-\kappa(a^\dagger a\rho-2a\rho a^\dagger+\rho a^\dagger a)-\gamma_{21}(S^+S^-\rho-2S^-\rho S^++\rho S^+S^-)$$
$$-\gamma_{12}(S^-S^+\rho-2S^+\rho S^-+\rho S^-S^+)-\Gamma(S^zS^z\rho-2S^z\rho S^z+\rho S^zS^z)\ , \tag{1}$$

where $\delta(=\omega_0-\omega_c)$ is the atom-cavity detuning, $2\gamma_{12}$ is the effective rate of pumping from lower to upper level, $2\gamma_{21}$ is the rate at which the upper level decays by spontaneous emission, Γ is the decay rate due to dephasing processes, and g is the atom-cavity coupling constant. The rotating-wave approximation was used in (1) while writing the atom-cavity interaction. Note that at optical frequencies, the effect of thermal photons is negligible and thus is not included in (1). We now concentrate on the infinite family of single time expectation values given by

$$\Psi_p^{(1)}=\langle(a^\dagger)^pa^p\rangle\ , \tag{2}$$
$$\Psi_p^{(2)}=\langle(a^\dagger)^pa^pS^z\rangle\ , \tag{3}$$
$$\Psi_p^{(+)}=\langle S^+(a^\dagger)^{p-1}a^p+S^-(a^\dagger)^pa^{p-1}\rangle\ , \tag{4}$$
$$\Psi_p^{(-)}=i\langle S^+(a^\dagger)^{p-1}a^p-S^-(a^\dagger)^pa^{p-1}\rangle\ . \tag{5}$$

On using the master equation (1) we find time-evolution equations for the expectation values

$$\dot\Psi_p^{(1)}=gp\Psi_p^{(-)}-2\kappa p\Psi_p^{(1)}\ , \tag{6}$$

$$\dot\Psi_p^{(2)}=-g\frac{p}{2}\Psi_p^{(-)}-g\Psi_{p+1}^{(-)}-2(\kappa p+\gamma_{21}+\gamma_{12})\Psi_p^{(2)}$$
$$+(\gamma_{21}-\gamma_{12})\Psi_p^{(1)}\ , \tag{7}$$

$$\dot\Psi_p^{(+)}=\delta\Psi_p^{(-)}-[\kappa(2p-1)+\gamma_{21}+\gamma_{12}+\Gamma]\Psi_p^{(+)}\ , \tag{8}$$

$$\dot\Psi_p^{(-)}=+4g\Psi_p^{(2)}+2gp\Psi_{p-1}^{(2)}+gp\Psi_{p-1}^{(1)}-\delta\Psi_p^{(+)}$$
$$-[\kappa(2p-1)+\gamma_{21}+\gamma_{12}+\Gamma]\Psi_p^{(-)}\ . \tag{9}$$

Note that in the absence of detuning, instead of Eqs. (6)–(9) one can obtain three coupled equations with respect to $\Psi_p^{(1)}$, $\Psi_p^{(2)}$, and $\Psi_p^{(-)}$. The set of equations (6)–(9) is exact in the sense that it accounts for all possible decay phenomena and is valid for all coupling strengths (i.e., for any value of g). In this paper we focus our attention only on the steady-state behavior. In the steady-state limit, the set of equations (6)–(9) can be reduced to a scalar three-term recursion relation for the expectation values $\Psi_p^{(1)}$

$$c_p\Psi_p^{(1)}+d_p\Psi_{p+1}^{(1)}+e_p\Psi_{p-1}^{(1)}=0\quad\text{for } p\geq 2\ , \tag{10}$$

$$c_0\Psi_0^{(1)}+d_0\Psi_1^{(1)}=-e_0 \ . \tag{11}$$

Here the p-dependent coefficients c_p, d_p, e_p for $p=0,1,2,\ldots,$ are given by

$$c_p=\tilde{g}^2\left[\frac{\tilde{\gamma}_{12}-\tilde{\gamma}_{21}-p}{p+\tilde{\gamma}_{12}+\tilde{\gamma}_{21}}-\frac{p}{p-1+\tilde{\gamma}_{12}+\tilde{\gamma}_{21}}\right] -(2p-1+\tilde{\gamma}_{12}+\tilde{\gamma}_{21}+\tilde{\Gamma}) \times\left[1+\frac{\tilde{\delta}^2}{2p-1+\tilde{\gamma}_{12}+\tilde{\gamma}_{21}+\tilde{\Gamma}}\right], \tag{12}$$

$$d_p=-\frac{2\tilde{g}^2}{p+\tilde{\gamma}_{12}+\tilde{\gamma}_{21}} \ , \tag{13}$$

$$e_p=\frac{\tilde{g}^2\tilde{\gamma}_{12}}{p-1+\tilde{\gamma}_{12}+\tilde{\gamma}_{21}} \ . \tag{14}$$

In Eqs. (12)–(14) the tilda denotes the respective quantities normalized with respect to the cavity damping κ.

The recursion relation (10) with the condition (11) can be solved for $\Psi_p^{(1)}$ ($p=1,2,3,\ldots,$) using the standard continued-fraction techniques.[10] Other physical quantities $\Psi_p^{(2)}$ and $\Psi_p^{(\pm)}$ can then be evaluated using Eqs. (6)–(8). We investigate the steady-state dependence of the following quantities on the system parameters.

(a) $\Psi_1^{(1)}=\langle a^\dagger a\rangle$, (15)

(b) $\Psi_0^{(2)}+\frac{1}{2}=\langle S^z\rangle+\frac{1}{2}$, (16)

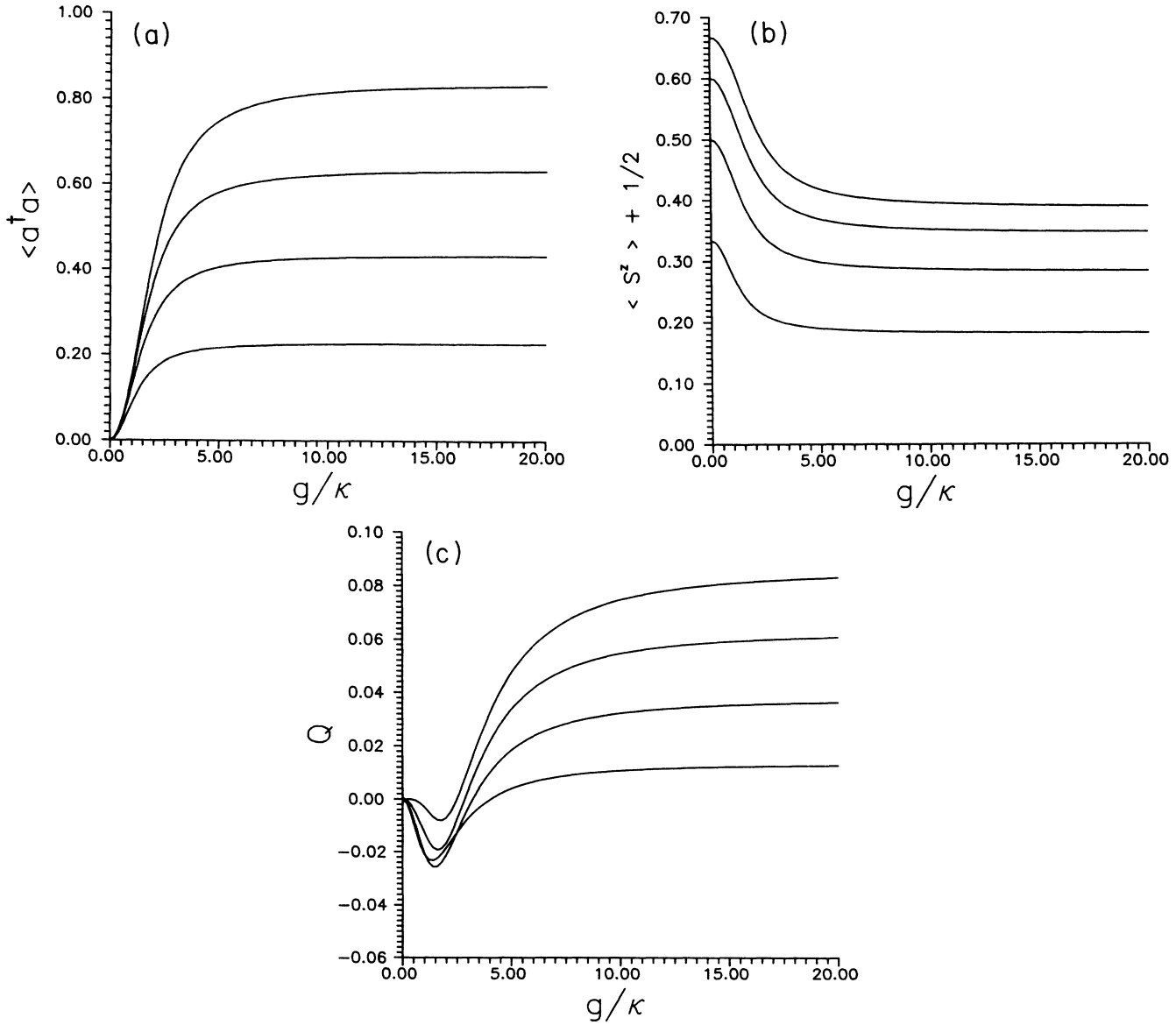

FIG. 2. (a) $\langle a^\dagger a\rangle$, (b) Q, and (c) C as functions of g/κ for $\gamma_{21}/\kappa=10$ and for $\gamma_{12}/\kappa=5$, 10, and 15. Curves from bottom to top in (a) and (b) are for increasing values of γ_{12}/κ, whereas in (c) they are for decreasing values.

(c) $$Q=\frac{\langle (a^\dagger)^2 a^2\rangle-\langle a^\dagger a\rangle^2}{\langle a^\dagger a\rangle}\ , \tag{17}$$

(d) $$C=\langle a^\dagger a S^z\rangle-\langle a^\dagger a\rangle\langle S^z\rangle\ , \tag{18}$$

It is evident that the first two quantities give, respectively, the average photon number and the excited-state population. The third one determines the nature of statistics of the cavity photons. Depending on whether Q is larger or smaller than zero, the statistics is super- or sub-Poissonian. Finally, the fourth and last one gives the atom-field correlation. In what follows we present the results of our numerical calculations. Calculations have been performed for two values of normalized spontaneous decay $\tilde{\gamma}_{21}$, namely, $\tilde{\gamma}_{21}=\gamma_{21}/\kappa=1$ and 10, and in all the calculations Γ has been set equal to zero. In Figs. 1(a)–1(c) we present the results for the resonant case (for $\delta=0$) and when $\tilde{\gamma}_{21}=1$. We have plotted the photon number, the excited-state population, and the Q parameter as functions of normalized coupling $\tilde{g}=g/\kappa$ in Figs. 1(a), 1(b), and 1(c), respectively. The various curves in each of these figures are for increasing values of the normalized pump rate $\tilde{\gamma}_{12}$ from 0.5 to 2 in steps of 0.5. It is clear from Fig. 1(a) that for fixed pumping of the upper atomic level and increasing $\tilde{g}$, the number of photons increase monotonically and saturates for large coupling. It is also obvious that the larger the value of $\tilde{\gamma}_{12}$, the larger is the saturation value of $\langle a^\dagger a\rangle$. In fact, for very large coupling, $\langle a^\dagger a\rangle$ shows an approximately linear increase with $\tilde{\gamma}_{12}$. The behavior of the curves in Fig. 1(b) is opposite that shown in Fig. 1(a) since the upper-level popula-

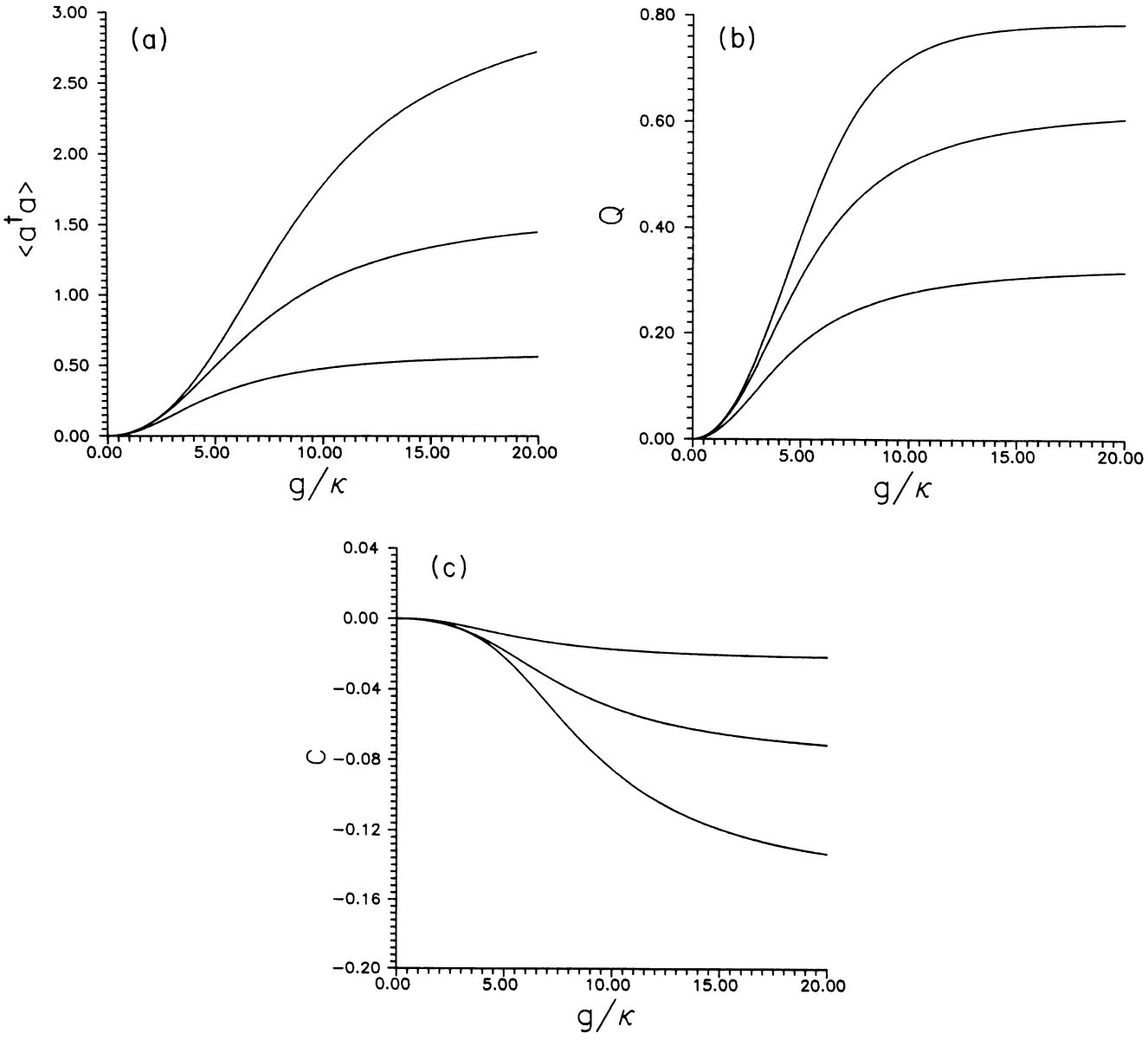

FIG. 2. (a) $\langle a^\dagger a\rangle$, (b) Q, and (c) C as functions of g/κ for $\gamma_{21}/\kappa=10$ and for $\gamma_{12}/\kappa=5$, 10, and 15. Curves from bottom to top in (a) and (b) [(c)] are for increasing values of γ_{12}/κ.

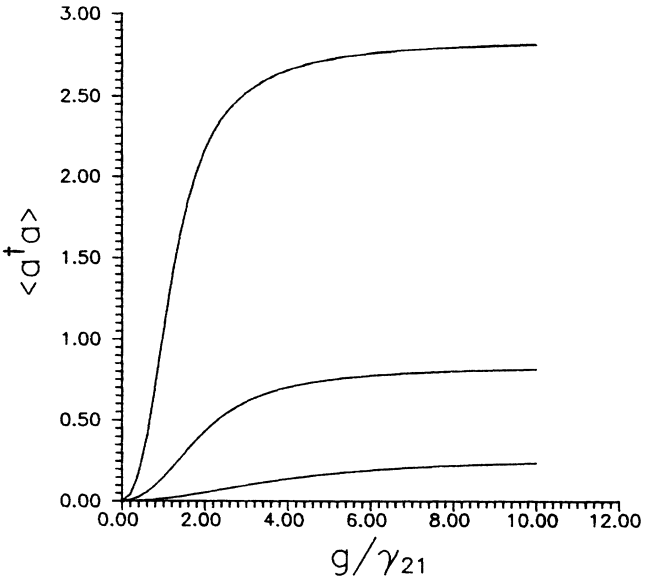

FIG. 3. $\langle a^\dagger a \rangle$ as a function of g/γ_{21} for $\gamma_{12}/\gamma_{21}=2$. Curves from top to bottom are for $\kappa/\gamma_{21}=0.2$, 1, and 5.

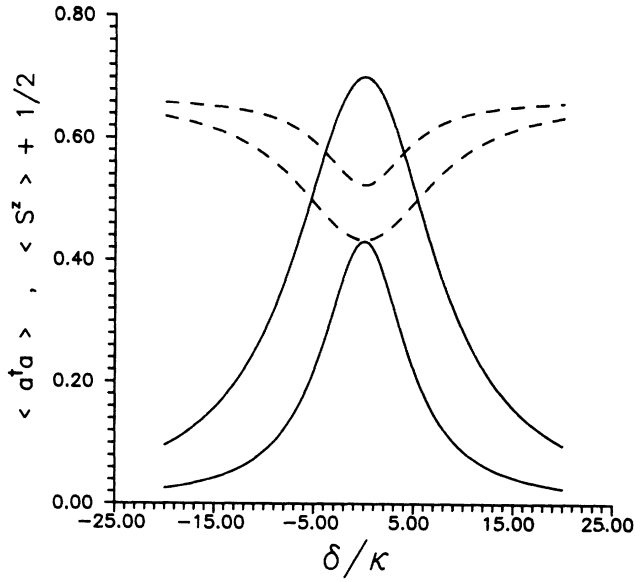

FIG. 4. $\langle a^\dagger a \rangle$ (solid line) and $\langle S^z \rangle + \frac{1}{2}$ (dashed line) as functions of normalized detuning δ/κ for $\gamma_{12}/\kappa=2$ and for $g/\kappa=2,4$. Upper (lower) curve corresponds to larger value of g/κ for $\langle a^\dagger a \rangle$ ($\langle S^z \rangle + \frac{1}{2}$).

tion falls monotonically with an increase in $\tilde{g}$. This implies that the excited state population, which is larger for larger pump, goes down so as to generate photons in the cavity. For larger coupling the population reduction is more effective, leading to a larger number of photons. The dependence of Q on normalized coupling $\tilde{g}$ [shown in Fig. 1(c)] is quite interesting in the sense that depending on the coupling strength the statistics can change from sub- to super-Poissonian. Besides, the sub-Poissonian character can be optimized by choosing the parameters (i.e., by selecting $\tilde{\gamma}_{21}$). Note that for $\tilde{\gamma}_{12}$ close to 1 [see Fig. 1(c)] the sub-Poissonian character is most pronounced. We now present the results for $\langle a^\dagger a \rangle$, Q, and C for $\tilde{\gamma}_{21}=10$. These are shown in Figs. 2(a), 2(b), and 2(c), respectively. Different curves in each of them are for three values of $\tilde{\gamma}_{12}$ from 5 to 15 in steps of 5. Figure 2(b) shows a super-Poissonian statistics for the field in contrast to the previous case [Fig. 1(b)] for smaller spontaneous decay, where a certain range of the coupling constant yields sub-Poissonian character. Finally, the atom-field correlation parameter C is plotted in Fig. 2(c). This figure shows a monotonic decrease of C as $\tilde{g}$ is increased. Note that for zero coupling there is no correlation between the atomic system and the radiation field, and the absolute value of this correlation increases with coupling. Note that the parameter C can be observed by studying the probability for simultaneous detection of the fluorescent photon and the cavity photon. This probability is proportional to $\langle a^\dagger a S^z \rangle$, whereas the probability will be proportional to $\langle a^\dagger a \rangle \langle S^z \rangle$ if there is *no* correlation.

In order to understand the steady-state behavior in good or bad cavity limits, we plot in Fig. 3 the photon number $\langle a^\dagger a \rangle$ for fixed $\gamma_{12}/\gamma_{21}(=2)$, as a function of g/γ_{21} for different values of κ/γ_{21}, namely, $\kappa/\gamma_{21}=0.2$, 1, and 5. It is clear from Fig. 3 that as the quality of the cavity is improved the number of photons increases. As a function of the coupling the average photon number shows the saturation behavior discussed earlier. Note also that the saturation is reached at smaller values of coupling in a good cavity. Finally, we investigate the dependence of the number of photons and the excited-state population of the normalized detuning $\tilde{\delta}$ for fixed $\tilde{\gamma}_{21}$ and $\tilde{\gamma}_{12}$ and for two different values of $\tilde{g}$, namely, $\tilde{g}=2,4$. The results are shown in Fig. 4, where the solid (dashed) lines are for $\langle a^\dagger a \rangle$ ($\langle S^z \rangle + \frac{1}{2}$). Figure 4 clearly indicates that larger coupling leads to a stronger depletion of the upper-level population leading to a larger number of photons. Besides, the frequency response is broadened as the coupling is increased. In most of our calculations we have increased the value of $\tilde{g}$ up to 20. The convergence of the matrix continued fraction for such large values of coupling was rather fast.

In conclusion, we have investigated an optical cavity with an atom pumped incoherently in the presence of all possible decay phenomena and presented exact results (without any approximations on the system parameters) on the growth of the cavity field, photon statistics and the excited-state population.

One of us (G.S.A.) would like to thank the Department of Science and Technology, Government of India, for partially supporting this work and L. Lugiato for an interesting discussion.

[1]S. Haroche and J. M. Raimond in *Advances in Atomic and Molecular Physics,* edited by D. Bates and B. Bederson (Academic, New York, 1985), Vol. 20, p. 347.

[2]D. Meschede, H. Walther, and G. Miller, Phys. Rev. Lett. **54**, 551 (1985); G. Rempe, H. Walther, and N. Klein, Phys. Rev. Lett. **58**, 353 (1987).

[3]Y. Zhu, A. Lezama, T. W. Mossberg, and M. Lewenstein, Phys. Rev. Lett. **61**, 1946 (1988).

[4]J. J. Sanchez-Mondragon, N. B. Narozhny, and J. H. Eberly, Phys. Rev. Lett. **51**, 550 (1983).

[5]G. S. Agarwal, Phys. Rev. Lett. **53**, 1732 (1984).

[6]G. S. Agarwal, R. K. Bullough, and G. P. Hildred, Opt. Commun. **59**, 23 (1986).

[7]G. V. Varada, M. Sanjay Kumar, and G. S. Agarwal, Opt. Commun. **62**, 328 (1987).

[8]M. J. Raizen, R. J. Thompson, R. J. Brecha, H. J. Kimble, and H. J. Carmichael, Phys. Rev. Lett. **63**, 240 (1989).

[9]F. DeMartini and G. R. Jacobovitz, Phys. Rev. Lett. **60**, 1711 (1988); F. DeMartini, G. Innocenti, G. R. Jacobovitz, and P. R. Mataloni, Phys. Rev. Lett. **59**, 2955 (1987).

[10]Continued-fraction methods were used first in the context of cavity QED in Ref. 6.